

The COVID-19 lockdown induced changes of SO₂ pollution in its Human-made global hotspots



Amritha S ^{a,b}, Patel VK ^c, Kuttippurath J ^{c,*}, Varikoden Hamza ^b

^a Department of Physical Oceanography, Kerala University of Fisheries and Ocean Studies, Kochi, India

^b Indian Institute of Tropical Meteorology, Ministry of Earth Sciences, Pune, India

^c CORAL, Indian Institute of Technology Kharagpur, Kharagpur, 721302, India

ARTICLE INFO

Article history:

Received 7 April 2024

Received in revised form

4 June 2024

Accepted 19 June 2024

Available online 27 June 2024

Keywords:

Sulphur dioxide

COVID-19

Natural anthropause

Coal usage

Global

Air pollution

ABSTRACT

Sulphur dioxide (SO₂) is a hazardous air pollutant, which is mostly emitted from burning of fossil fuels, and has an adverse impact on the human health and ecosystem functioning. The COVID-19 natural anthropause (lockdown) provides a great opportunity to understand the changes in SO₂ pollution across the globe, as there was a temporary standstill for most human activities. Therefore, we analyse the changes in global SO₂ pollution during lockdown compared to pre-lockdown and identify its hotspots driven by human activities using satellite measurements, reanalysis data and emission inventory. We observe a decline in SO₂ pollution of about 2.21 % in its global average, -21.05 % in Indo-Gangatic Plain, -16 % in East China, -7.67 % in East United States of America, -3.99 % in Western Europe and -3.85 % in Middle East owing to the halt in human activities such as industrial and transport operations, as found from the emissions inventory. There are point and aerial hotspots of SO₂ pollution across the globe (e.g. cities or industrial units), which also show a decrease (20–30 %) in SO₂ pollution during the anthropause. Fossil fuel burning in thermal power plants is a major source of SO₂ pollution, and it has declined notably (1–12 %) during the lockdown in the major coal consuming countries such as the United States, China, Japan, Canada, Brazil, Australia, France, Germany, Spain, Italy and the United Kingdom. Therefore, lockdown provides a clear understanding of global human-driven hotspots of SO₂ pollution and their changes, which would help us to make better and effective air pollution mitigation strategies.

© 2024 The Authors. Publishing services by Elsevier B.V. on behalf of KeAi Communications Co. Ltd. This is an open access article under the CC BY-NC-ND license (<http://creativecommons.org/licenses/by-nc-nd/4.0/>).

1. Introduction

Sulphur dioxide (SO₂) is a short-lived hazardous gaseous air pollutant and is classified as a criteria pollutant by the Environmental Protection Agency (EPA). There are several adverse impacts of SO₂ pollution on human health and climate. For instance, high SO₂ pollution can cause negative impacts on environment such as the acid rain [1]. In addition, it also forms particulate matter through the oxidation process and can impact the regional and

global climate by altering the radiative forcing [2]. Furthermore, in addition to its influence on the climate, SO₂ pollution has the potential to aggravate respiratory conditions such as bronchitis. Additionally, it has the potential to bring on symptoms such as coughing, wheezing, phlegm and asthma attacks [1,3]. There are many sources of atmospheric SO₂ varying from natural to anthropogenic. Emissions from coal-based thermal power plants, refineries and fossil fuel burning are the typical examples of human driven SO₂ pollution [4,5]. On the other hand, emissions from volcanic activities and biomass burning are the natural sources. Therefore, it is important to understand the natural and human driven SO₂ pollution hotspots across the latitudes to implement effective mitigation strategies and policy measures. The COVID-19 lockdown (LD) measures can be considered as a natural experiment to differentiate the natural and man-made hotspots of SO₂ pollution as most anthropogenic activities were curtailed during this period.

* Corresponding author.

E-mail address: [\(K. J.\).](mailto:jayan@coral.iitkgp.ac.in)



Production and Hosting by Elsevier on behalf of KeAi

Developed countries have made a big progress in reducing anthropogenic SO₂ emissions by implementing stringent environmental regulations and adoption of advanced technologies [6,7]. Emissions of SO₂ pollution in developing countries are increasing in recent decades due to ineffective strategies to curb air pollution [8]. However, some developing countries have taken effective measures in recent years to combat air pollution. For example, SO₂ emissions in China have declined significantly since 2013 due to the Air Pollution Prevention and Control Action Plan [9]. Similarly, SO₂ pollution in India has declined in the past decade due to the implementation of control technology and environmental regulations [5]. As there were no strategic plan to curb air pollution, SO₂ pollution has shown rising trends in many other developing countries in the past decades; indicating also the growth of electricity demand there [8,10,11]. The energy security is one of the most important factors that determines the economic development of a country, but the generation of energy requires fossil fuels that degrade the environment, including air quality. However, both energy security and safe environmental conditions can be achieved simultaneously thorough the implementation of effective and sustainable technology in industries and by generating renewable energy [12]. The spatial distribution and hotspots of global SO₂ pollution have changed dramatically in recent years due to such divergent patterns in SO₂ emissions by different countries [13,14]. Most global SO₂ anthropogenic emissions are associated with socio-economic development such as those related to fossil fuels, power plants and other industrial activities. Nevertheless, these anthropogenic emissions were curtailed during LD, and this situation can help to identify their natural hotspots in the world.

The global spread of severe acute respiratory syndrome (SARS-CoV-2) has had a significant impact on economies, society, vehicular traffic, tourism and human connectivity. Meteorological factors such as winds played an important role in the spread of this virus. For instance, Coccia [15,16] reported that the regions or cities with low wind speed and high pollution had higher number of COVID-19 related mortality, while those with high wind speed have fewer number of COVID-19 cases. To limit the spread of the virus, the administrations in different countries imposed restrictions on various anthropogenic activities, which can also be termed as anthropause. However, the duration of LD was not the same or uniform in all countries and even within the countries [17–21]. Each phase had different impacts on economic activities, mortality rate and environmental conditions [18,22]. The COVID-19 LD also led to various environmental problems such as plastic pollution, waste generation, marine contamination of plastics and threat to the biodiversity, and are expected to persist as long-term challenges [23–25]. Currently, there is a lack of clarity regarding the methods to detect and assess the environmental impacts, and their consequences for future environmental management.

On the other hand, there was an improvement in air quality across the globe owing to the COVID-19 induced anthropause. For example, Kuttippurath et al. [22] found a decline in SO₂ pollution in Indian regions related to anthropogenic hotspots in the last decade. Similarly, there is a big reduction in SO₂ pollution in the cities of Turkey (59 %) during LD compared to previous years, which is primarily related to the restrictions in human mobility [26]. In addition, Çalik and Doğruparmak [27] found a decline in air pollutants, including SO₂ (6–17 %), in Turkey during LD compared to its previous year concentrations. Similarly, Akan and Coccia [28] found a notable improvement in SO₂ pollution in many countries, including China, France, Australia, Israel and Germany. They also noted that the decline in pollution depends on the geography, economy, industrial activities and social characteristics of individual countries. Furthermore, Ling and Li [29] found that SO₂ pollution has declined in China in view of LD, about 7.42 %, compared to

previous years. This decrease is mostly related to the temporary halt of human movement and economic activities. Wang et al. [30] found that LD along with air pollution control measures led to the improvement in air quality in the Guangdong-Hong Kong-Macao Greater Bay Area of China. Qayyum et al. [31] found a decline (59.1 %) in SO₂ pollution in the mega city of Lahore during LD compared to the same period in 2019. Kandari and Kumar [32] examined the impact of LD on air quality and found a remarkable improvement in SO₂ pollution in South Asian countries. The South Asian countries face various challenges due to poor air quality, and LD measures provided a temporary relaxation, as most pollutants declined significantly during the period there [33]. On a global scale, Venter et al. [34] and Navaratnam et al. [35] suggested that global air pollution has declined due to LD, but changes are not uniform among the countries.

Most of these studies discuss the environmental impact of LD, and only a few have quantified and compared its unintended environmental effects. However, LD measures provide an apt opportunity to understand the air pollution in different angles. For example, it is a new way of looking at anthropogenic and naturally driven pollution hotspots, which can aid in the formulation of environmental regulations. Therefore, we aim at understanding the anthropogenic and natural hotspots of SO₂ through the eyes of LD measures. We use satellite measurements, reanalysis data and emission inventory to understand the changes in global SO₂ pollution. First, we identify the hotspots of SO₂ pollution across the globe, and then estimate their changes during LD compared to that in the previous years. Second, we discuss the regions/hotspots driven by anthropogenic and natural sources using emission inventory. In addition, we also examine the changes in SO₂ pollution together with coal consumption in different countries, and assess the policy regulations that can be implemented to curb the SO₂ pollution.

2. Data and methods

2.1. Defining the lockdown period

The LD period varied globally depending on the country and therefore, we investigated the LD period for most countries to determine its duration. We then verified our results with additional data sources [17]. We considered a typical LD period when most cities were subjected to strict movement restrictions, to conduct a thorough analysis on a global scale. To ensure that the same standard (e.g. workplace closures and travel bans) is used within and among the cities and regions, the criterion is applied to define the stages of LD. A few cities must have followed the description of LD, as the restrictions to limit people movements and activities were reliant on quickly changing local and national responses to the pandemic. Here, we have considered April–May 2020 as the LD period, the same months in 2017–2019 as the pre-lockdown (PreLD) and those in 2021–2022 as the post-lockdown (PostLD) periods.

2.2. Data sources

The Modern-Era Retrospective analysis for Research and Applications, Version 2 (MERRA-2) is one of the most recent atmospheric reanalysis data and are the enhanced iteration of MERRA [36]. The assimilation of worldwide SO₂ into the MERRA-2 dataset has been facilitated through the utilisation of data obtained from several satellites and ground-based instruments at a spatial resolution of $0.5^\circ \times 0.625^\circ$. To understand the changes in SO₂ pollution on a small spatial scale (e.g. cities), we use the fine resolution data ($3.5 \times 5.5 \text{ km}^2$) from TROPOspheric Monitoring Instrument

(TROPOMI) for the period 2019–2021, which is on board the Sentinel-5 Precursor satellite [37]. Negative vertical columns are frequently observed in clean areas and locations with very low SO₂.

The annual mean SO₂ source emission inventory is sourced from the Emission Database for Global Atmospheric Research version 8.1 (EDGAR_v8.1). It is a comprehensive and worldwide database that encompasses anthropogenic emissions of greenhouse gases and air pollutants, employing the bottom-up approach [38]. The EDGAR offers comprehensive data on emissions, presenting both national totals and grid maps at a global resolution of 0.1° × 0.1°, for the period from 1970 to 2022, but do not account for the emissions due to land use change.

The burnt area is examined with Ocean and Land Colour Instrument (OLCI) v 1.1 at a grid scale 0.25° × 0.25° for the period 2017–2022 to understand the changes of SO₂ in the areas of biomass and agricultural waste burning. These data are acquired by analysing variations in reflectance using medium resolution sensors, namely Moderate Resolution Imaging Spectroradiometer (MODIS) on Terra and Sentinel-3 OLCI. Additionally, the MODIS thermal information is utilised to support the analysis. The data of burned areas also include information pertaining to the land cover that has undergone burning. The implementation of LD does not have a direct influence on areas that are not affected by human activities. However, the seasonal variability in burned biomass can provide information on SO₂ emissions in those regions. In addition, we also use the MODIS land use class at 500 m spatial resolution to delineate forests and croplands for the attribution of biomass burning.

2.3. Measures of variables

We examine the changes in both total column and surface concentration of atmospheric SO₂ using TROPOMI and MERRA-2 data, respectively. These are considered on a monthly scale for April and May for the period 2017–2022. The changes in atmospheric SO₂ across the globe and its hotspots are investigated here. Furthermore, SO₂ emissions from the total anthropogenic activities is analysed using the EDGAR inventory for the period 2015–2019 to examine its anthropogenic hotspots, as most human activities were curtailed during LD. Furthermore, to understand the changes in SO₂ pollution on small spatial scales, we selected 3000 cities across the latitudes. These cities are distributed in all continents, and some of

them are the major urban centres of the world. We selected the cities because the LD measures were more effective there, in which the anthropogenic activities such as road transport and industrial operations are most dominant. To find the regions with natural emissions like biomass burning, we analyse the distribution of forest fires with burnt area. The fossil fuel burning in coal-based thermal power plants and oil and refinery industries are the major anthropogenic sources of atmospheric SO₂. Therefore, to understand the regions dominated by SO₂ pollution from anthropogenic activities, we also identify the location of large capacity thermal power plants and, oil and refinery industries in the world. The coal consumption in the major coal consuming countries in the world such as South Africa, the United States, China, India, Australia, Canada, Brazil, Russia, the United Kingdom, France, Germany, Spain, Italy, Japan, Indonesia and Mexico is also analysed for the period 2017–2020. SO₂ emissions from road transport, manufacturing and construction industries, energy and heat power generation, residential emissions and refinery industries are assessed to understand the contribution of anthropogenic activities to SO₂ pollution in these countries.

2.4. Data analysis

The SO₂ pollution hotspots across the latitudes are found based on both surface mass concentration and total column data taken from MERRA-2 and TROPOMI, respectively (Fig. 1). Among the regions East China (EC), Indo-Gangetic Plain (IGP), East USA, Western Europe (WE), South Africa (SA) and Middle East (MDE) are the major hotspots. The calculation of percentage changes in SO₂ pollution during LD is performed by comparing the average SO₂ observed in the years 2017–2019 and 2021–2022 for the respective months of LD period (April–May) in 2020. As TROPOMI data are available from 2018 onwards, we have considered 2018–2019 as PreLD, 2020 as LD and 2021–2022 as PostLD using the following relation:

$$\% Y_{LD} = \frac{Y_{LD} - Y_{PreLD/PostLD}}{Y_{PreLD/PostLD}} \times 100$$

$$\% Y_{PostLD} = \frac{Y_{PostLD} - Y_{LD}}{Y_{LD}} \times 100$$

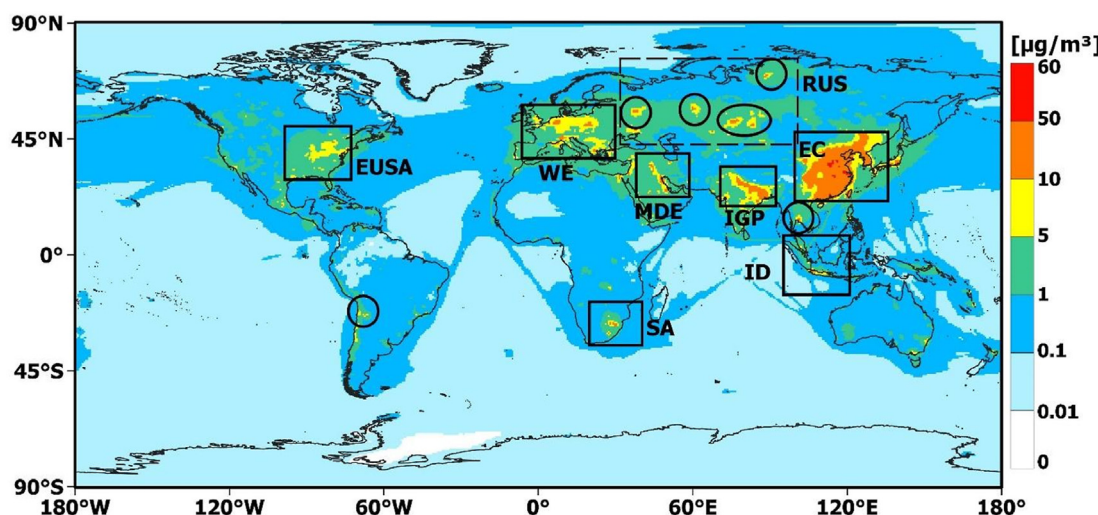


Fig. 1. Distribution of SO₂ surface mass concentration derived from MERRA-2 for the period 2000–2019. Regions such as East United States of America (EUSA), Western Europe (WE), Middle East (MDE), Indo-Gangetic Plain (IGP), Indonesia (ID), East China (EC), Russia (RUS) and South Africa (SA) are the hotspots of SO₂.

Where Y is the amount of atmospheric SO₂.

These computations are conducted for all regions, cities and countries. In addition, a comparative analysis for the LD, PreLD and PostLD periods is also performed for the SO₂ emissions from energy and heat power generation, manufacturing and construction industries, road transport, residential, and refinery industries together with the coal consumption and gross domestic product (GDP) for the mentioned countries. Note that, we have taken a shorter period for PreLD and PostLD to avoid the influence of long-term trends. The identification of hotspots, whether driven by anthropogenic or natural factors, is accomplished through finding the temporal changes and using the inventory, geographical location of anthropogenic activities and changes in coal consumption. In addition, we also analyse the contribution of SO₂ emission from road transport, energy and heat power generation, refinery industries, and manufacturing and construction industries to the total anthropogenic activities for the mentioned countries using following relation:

$$\% X_{\text{contribution}} = \frac{X_{\text{RT,EHP,MIC,REF Emission}}}{X_{\text{Total Emission}}} \times 100$$

Where, $X_{\text{RT,EHP,MIC,REF Emission}}$ indicates SO₂ emissions from road transport (RT)/energy and power generation (EHP)/manufacturing and construction industries/refinery. $X_{\text{contribution}}$ indicates percentage contribution of SO₂ emission from different sectors to the total anthropogenic emissions ($X_{\text{Total Emission}}$). We select these sectors as they are mostly affected by the LD measures. The detailed methodology flow chart is given in Supplementary material (Fig. S1).

As total anthropogenic SO₂ emissions data from EDGARv8.1 are available on annual scale, we computed the changes in emission by considering 2020 (LD year), 2017–2019 (before, PreLD) and 2021–2022 (after, PostLD). Also, the coal consumption and GDP data are extracted as yearly mean for the same period, and change is computed as:

$$\% Z_{2020(2021-2022)} = \frac{X_{2020(2021-2022)} - Y_{2017-2019(2020)}}{Y_{2017-2019(2020)}} \times 100$$

Where Z is the total anthropogenic SO₂ emission/coal consumption/GDP.

Furthermore, to understand the link between sectoral SO₂ emissions, SO₂ amount and GDP for the abovementioned countries, Pearson's correlation is performed for the period 2000–2022. The Pearson correlation indicates the link between two variables that are measured on a continuous scale. The assigned number ranges from –1 to 1, where 0 indicates no connection, 1 shows a complete positive correlation, and –1 suggests an absolute inverse relationship. The correlation coefficient is computed for a pair of parameters (e.g. x and y) by adding the products of their deviations from their respective averages (e.g. x_{mean} and y_{mean}) and then dividing it by the product of the squared deviations from their respective means

$$\text{Pearson Correlation Coefficient} = \frac{\sum (x_i - x_{\text{mean}})(y_i - y_{\text{mean}})}{\sqrt{\sum (x_i - x_{\text{mean}})^2} \sqrt{\sum (y_i - y_{\text{mean}})^2}}$$

3. Results and discussion

3.1. The global SO₂ pollution hotspots

To identify the hotspots, we analyse the annual climatology of global atmospheric SO₂ for the period 2010–2020, as shown in Fig. 1. Most hotspots of SO₂ pollution are in the northern hemisphere, where human activities are predominant. For example, East China (EC), Indo-Gangatic Plain (IGP), Western Europe (WE), East United States of America (EUSA) and Middle East (MDE) are the largest hotspots of SO₂ pollution, with values greater than 5 µg/m³. On the other hand, South Africa (SA) is the major hotspot of SO₂ pollution in the southern hemisphere. Note that there are point hotspots across the globe, which can be cities (e.g. New Delhi, Riyadh and Beijing) or industrial clusters (e.g. Eastern North America and Western and Central Europe). For instance, there are various point sources in Russia, South America, North America, Southeast Asia and Australia, and some are shown in Fig. 1. Both human-made factors, including industrial processes, and natural events such as biomass burning, wildfires and volcanic activity collectively contribute to the release of SO₂ in these hotspots [5,39,40]. The highest amount of SO₂ is in EC, about >10 µg/m³. About 90 % of SO₂ emissions in China is from the burning coal, and oil and other fuel sources [41,42]. Like EC, IGP and WE, some regions in MDE exhibit high values of SO₂, which makes its pollution hotspots, and are attributed to the anthropogenic sources [43,44]. Column SO₂ derived from satellite measurements also shows similar hotspots, as found from the surface concentration (Fig. S2). For example, the hotspots in the northern hemisphere are IGP, EC, WE, some areas in MDE and the USA, with values >25 × 10⁻⁵ mol/m². Similarly, SA, southern areas in South America and the southeastern Australia are the major hotspots in the southern hemisphere.

Among the anthropogenic activities, burning coal for power generation is one of the largest sources of SO₂ pollution [4,5,45]. In addition, other anthropogenic activities like vehicular emissions, manufacturing processes and agriculture waste burning (AWB) also contribute to the total SO₂ emissions, depending on the region [5,46,47]. In contrast, the natural processes like volcanic emissions or forest fires add significantly to the total SO₂ emissions [39,48]. Distribution of SO₂ emissions from the total anthropogenic activities are shown in Fig. S3. There are very high values of total anthropogenic emissions of SO₂ in the hotspots of IGP, EC and SA, about >45 × 10⁻¹² kg/m²/s. Other regions also exhibit high anthropogenic emissions. For instance, some regions in the USA and MDE, including cities (e.g. Washington D. C., New York, San Francisco, Los Angeles, Boston, Riyadh, Doha and Kuwait) or industrial regions (e.g. Salt Lake City, Eastern Texas, Detroit and Chicago), and hotspots in Russia (e.g. Noril'sk and Moscow) show very high value of SO₂ emissions, about >50 × 10⁻¹² kg/m²/s. In Central Africa, Amazonia and some regions in Siberia show either zero or very small values of total anthropogenic SO₂ emissions, <5 × 10⁻¹² kg/m²/s, indicating the natural sources like forest fires or wildfires there.

We also analyse the temporal evolution of atmospheric SO₂ in its hotspots across the globe during LD (April–May), as shown in Fig. S4. There is a gradual rise in SO₂ pollution in IGP, EC and in the

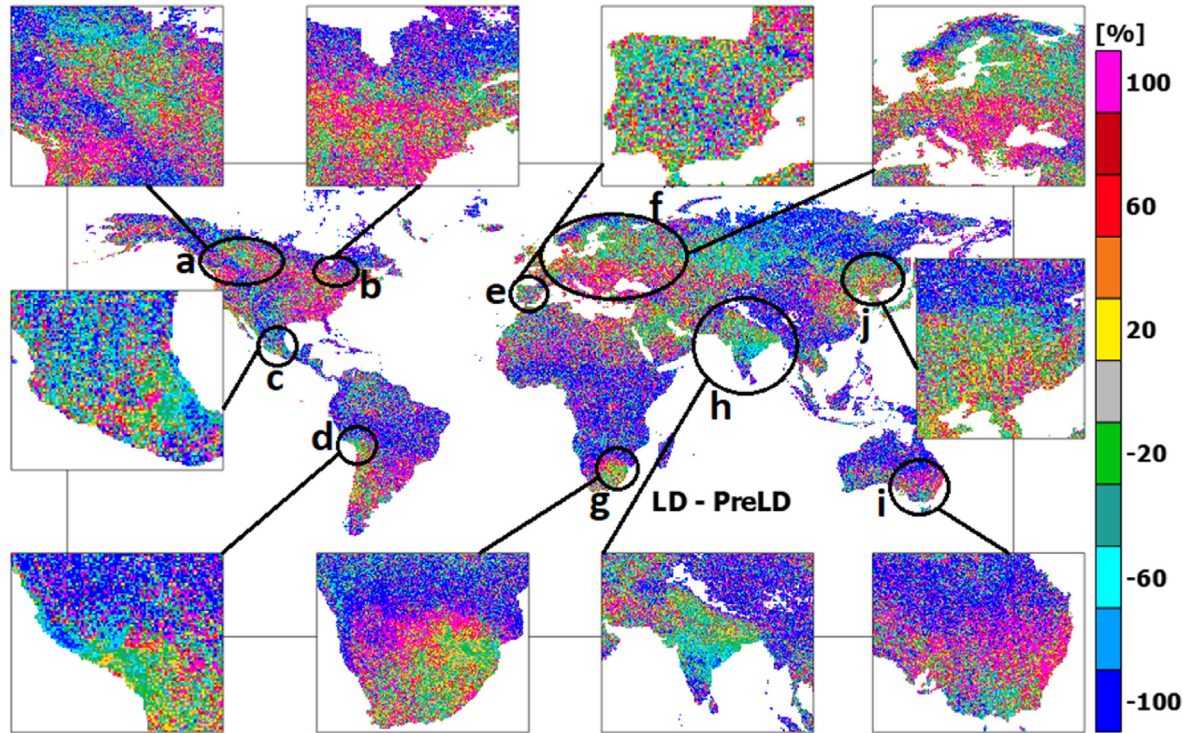


Fig. 2. Changes in SO₂ during lockdown (LD: April–May 2020) compared to its pre-lockdown (PreLD: April–May 2017–2019) derived from the TROPOMI satellite measurements. Here, regional changes are projected for western Canada (a), eastern Canada (b), Mexico (c), regions in western South America (d), Spain (e), Western Europe (f), South Africa (g), India (h), Southeast Australia (i) and Northeast China (j).

Table 1

Changes in SO₂ surface mass concentration derived from MERRA-2 during lockdown (LD) compared to pre-lockdown (PreLD) and post-lockdown (PostLD) in the global average and hotspots.

Hotspots	LD - PreLD	PostLD - LD
Indo-Gangetic Plain	-21.1 %	12.2 %
East China	-16 %	-1.4 %
Middle East	-3.8 %	7.6 %
East USA	-7.6 %	4.9 %
Western Europe	-3.9 %	-11.9 %
South Africa	-18 %	-5.4 %
Australia	-31.4 %	30.3 %
Global Average	-2.2 %	1.9 %

global average until 2010, and it remains nearly constant thereafter. Similarly, a growth in SO₂ in the hotspots of SA and Australia is also observed. On the other hand, a gradual decline in SO₂ pollution is observed in the USA and WE owing to the stringent environmental regulations and technologies. Most hotspot regions show a drop in SO₂ pollution during LD, e.g., its global average shows a decline in the year 2020. Similarly, a reduction of SO₂ pollution is also observed in the eastern USA, MDE, SA and Australia in 2020. A stronger drop in SO₂ pollution is observed in the hotspots of Australia. In contrast, a small rise of SO₂ pollution is observed in WE during LD. As we have considered the area averaged values of SO₂, the impact of LD may not be completely visible in these data. Therefore, we have quantitatively analysed the changes in atmospheric SO₂ during LD compared to PreLD and PostLD on different spatial and temporal scales.

3.2. Changes in SO₂ pollution during LD compared to PreLD and PostLD

Prior to LD, there was a widespread and severe issue of high

urban air pollution in the world, particularly due to SO₂, NO₂ and particulate matter [19,21,22,49]. The primary contributors to this pollution are transportation, industries and power stations [1,50]. As the countries implemented LD measures, industrial activities came to a global standstill. Among the affected sectors, transportation suffered the most due to LD [50–52]. Fig. 2 illustrates the changes in column SO₂ during LD compared to PreLD, indicating a reduction in its values in various regions. For instance, IGP and central parts of India, Myanmar and Thailand experience a substantial decrease of column SO₂, about 18–30 %. Furthermore, Tajikistan, Nepal, Kyrgyzstan and the MDE countries (e.g. Jordan, Kuwait, Iran, Turkey and the United Arab Emirates), Mexico, WE (e.g. areas in Spain) and some areas in the USA, particularly in the western and central USA, exhibit reductions of about 10–30 %. Additionally, point hotspots marked in Fig. 1, also show a significant decrease of SO₂ in a similar range. A comparable reduction in surface concentration of SO₂ is also observed in most hotspots during LD compared to PreLD (Fig. S5 and Table 1), as demonstrated by its 10–20 % cut in some areas of WE, MDE, Mexico, Australia, IGP, the eastern USA, SA and Russia. We also averaged the change in SO₂ in the hotspots, and found a peculiar pattern (Table 1). For example, a reduction in SO₂ is observed in MDE (3.85 %), East USA (7.67 %) and Australia (31.4 %). A similar decline in SO₂ is also observed in global average, about 2.21 %. However, a slight increase in SO₂ is observed in IGP (1.05 %), EC (1.08 %) and SA (0.88 %) during LD compared to PreLD.

To understand the changes in SO₂ pollution on smaller spatial scales, we have considered 3000 cities across the globe, as illustrated in Fig. 3. As cities are relatively small, we have considered the high spatially-resolved TROPOMI data to compute the changes during LD. We observe a decline (5–10 %) in SO₂ during LD compared to PreLD in major cities across India, including Chennai, Delhi, Kolkata, Bangalore and Mumbai. In North America, cities in

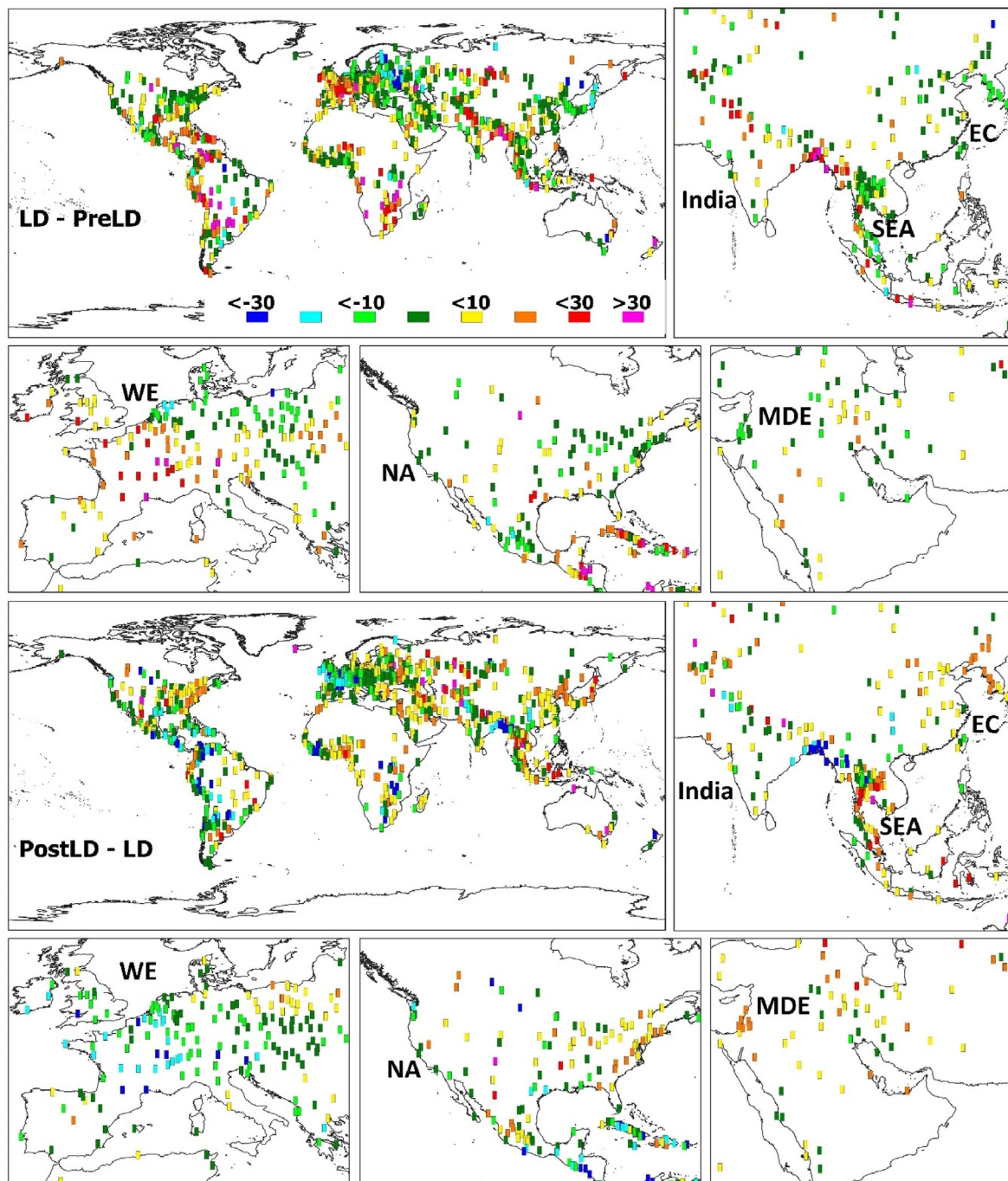


Fig. 3. Changes in SO₂ concentrations in 3000 major cities in the world during lockdown (LD: April–May 2020) compared to pre-lockdown (PreLD: April–May 2017–2019) and post-lockdown (PostLD: April–May 2021–2022) periods. Here, the regions are India, Southeast Asia (SEA), East China (EC), North America (NA), Middle East (MDE) and Western Europe (WE).

the East USA (e.g. New York, Charleston, Indianapolis, Jefferson City, St. Louis and Washington) and Mexico (e.g. Tampico, Aguascalientes, Guadalajara, Durango and Culiacan) exhibit a decrease in SO₂, about 5–25 %. A similar reduction is also found in MDE (Muscat, Al Mukalla, Lahij, Aden, Abu Dhabi and Al Kasab), Western Europe (e.g. Madrid, Braganca, Guarda, Arnhem, Ostersund, Hermansverk, Drammen and Haarlem), Russia (Skytyvkar, Smolensk, Klintsy, Tura and Igarka) and China (e.g. Luoyang, Baotou, Zhengzhou, Jinan, Tiayuan, Fuzhou and Chengdu) cities, reflecting the overall improvement in global SO₂ pollution. On the other hand,

the highest reduction of about 10–40 % is observed in many cities in the world, and some of them are Sendai, Nagoya, Kyoto, Kobe, Osaka, Gifu, Canberra, Melbourne, Jambi, Medan, Johannesburg, Bisho, Brasilia, Cuiaba, Sao Paulo, Santos, Duranzo, Trinidad, Rivera, Tacuarembó, Florida, Minas and Rosario.

To further understand the impact of LD on the anthropogenic activities and associated SO₂ pollution, we analyse its changes during LD with respect to PostLD, as depicted in Fig. S6. As restrictions were lifted during PostLD, we observe an increase in SO₂ pollution in most regions. For example, there is an increase in SO₂ in

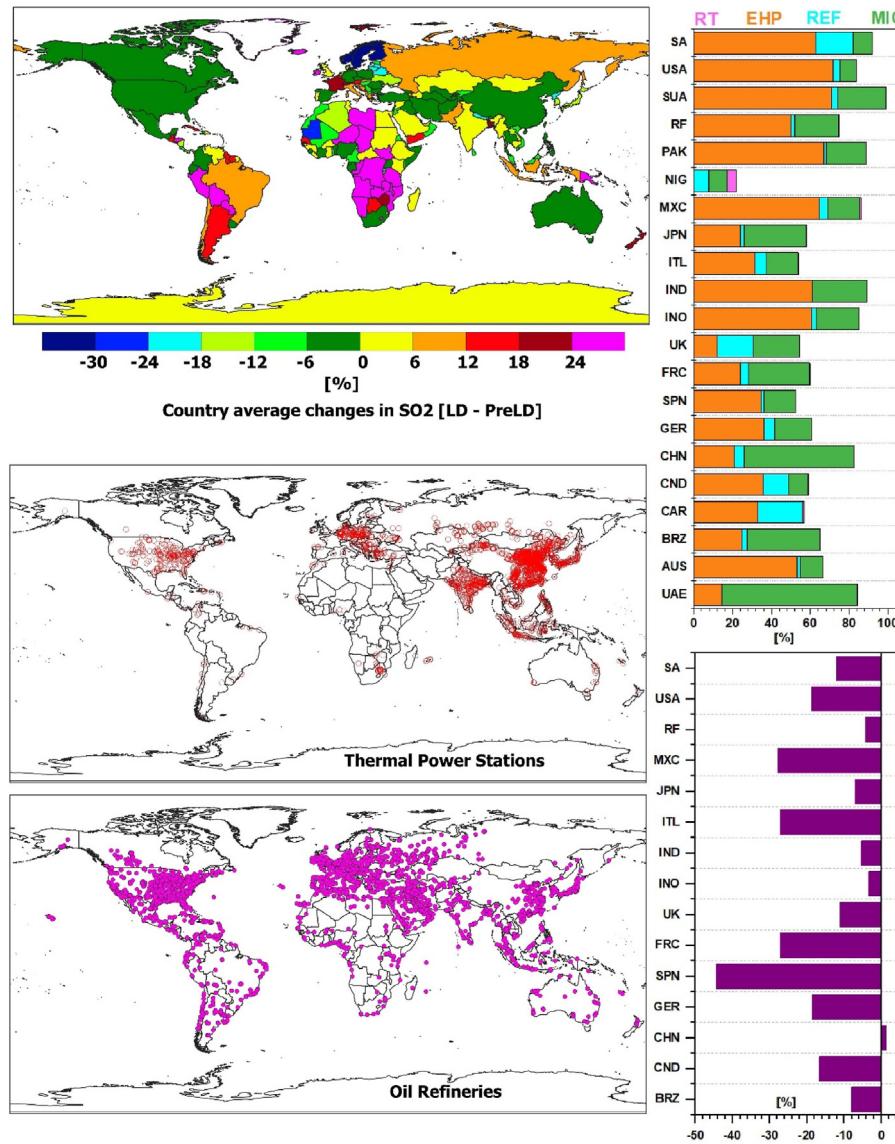


Fig. 4. Country average changes in atmospheric SO₂ during lockdown (LD) compared to pre-lockdown (PreLD: left top panel) derived from satellite measurements. Left middle and bottom panels represent geographical location of thermal power station and oil refineries. Right top panel shows the contribution of SO₂ emissions from road transport (RT), energy and heat power generation (EHP), refineries (REF), and manufacturing and construction industries (MIC) to the total anthropogenic emissions in all major coal consumer countries (country code with full name is given in Table S1).

the hotspots of Mexico, EUSA, SA, India, Australia, South Africa, WE, Russia and MDE, about >18 %. Increase in SO₂ pollution is also found at the surface in the above-mentioned hotspots (Fig. S7), except the western South America and South Africa, where its reduction >10 % is observed. The changes of SO₂ pollution in cities during PostLD are depicted in Fig. 3. For example, cities in India like Gandhinagar, Ahmadabad, Mumbai, Bhopal and Patna exhibit an increase of about 10–30 % during PostLD. Similarly, cities in the eastern USA such as Charlotte, Columbia, Richmond, Raleigh, Tallahassee, Des Moines, Jefferson and Indianapolis show a rise in SO₂ of about 10–20 % during PostLD. However, relatively smaller increase (about 5–10 %) in SO₂ is observed in St. Louis, Memphis, Pittsburgh, Columbus, Chicago, Frankfort, Springfield, Jacksonville, Charleston, Baltimore, Washington D.C., Brooklyn, Albany, Chester, New York and Boston. Cities in Mexico like Chihuahua, Culiacan, Durango, Zacatecas, Ciudad Victoria, Aguascalientes, Tepic, Guanajuato, Guadalajara, Queretaro, Morelia, Mexico City and Toluca exhibit an

increase in SO₂ of about 5–30 %. Alice Spring, Sydney, Adelaide, Melbourne, Hobart, Bandung, Yogyakarta, Jambi, Palembang, Huhot, Yinchuan, Lanzhou, Luoyang, Baotou, Chengdu, Wuhan, Nanjing, Beijing, Jinan, Tianjin, Tangshan show rise in SO₂ of about 5–20 %. In contrast, very high increase of about 20–30 % is observed in Wonsan, Hyesan, Kanggye, Hamhung, Palmas, Belo Horizonte, Ati, Mongo, Am Timan, El Kharga, Dongola, Wadi Halfa, El Fasher, Ostersund, Falun, Orebro, Karaganda, Karakol, Guarda, Syktyvkar, Salekhard, Urgench, Manzini, Mbabane and Halikulu. Many other cities in the world as depicted in Fig. 3 also exhibit an increase in SO₂ pollution during PostLD.

Here, we analyse the contribution of SO₂ emissions from energy and heat power generation, manufacturing and construction industry, road transport and refinery to the total anthropogenic emissions in major countries, where SO₂ pollution is very high compared to other countries in the world, as shown in Fig. 4. We observe that SO₂ emissions from energy and heat power generation

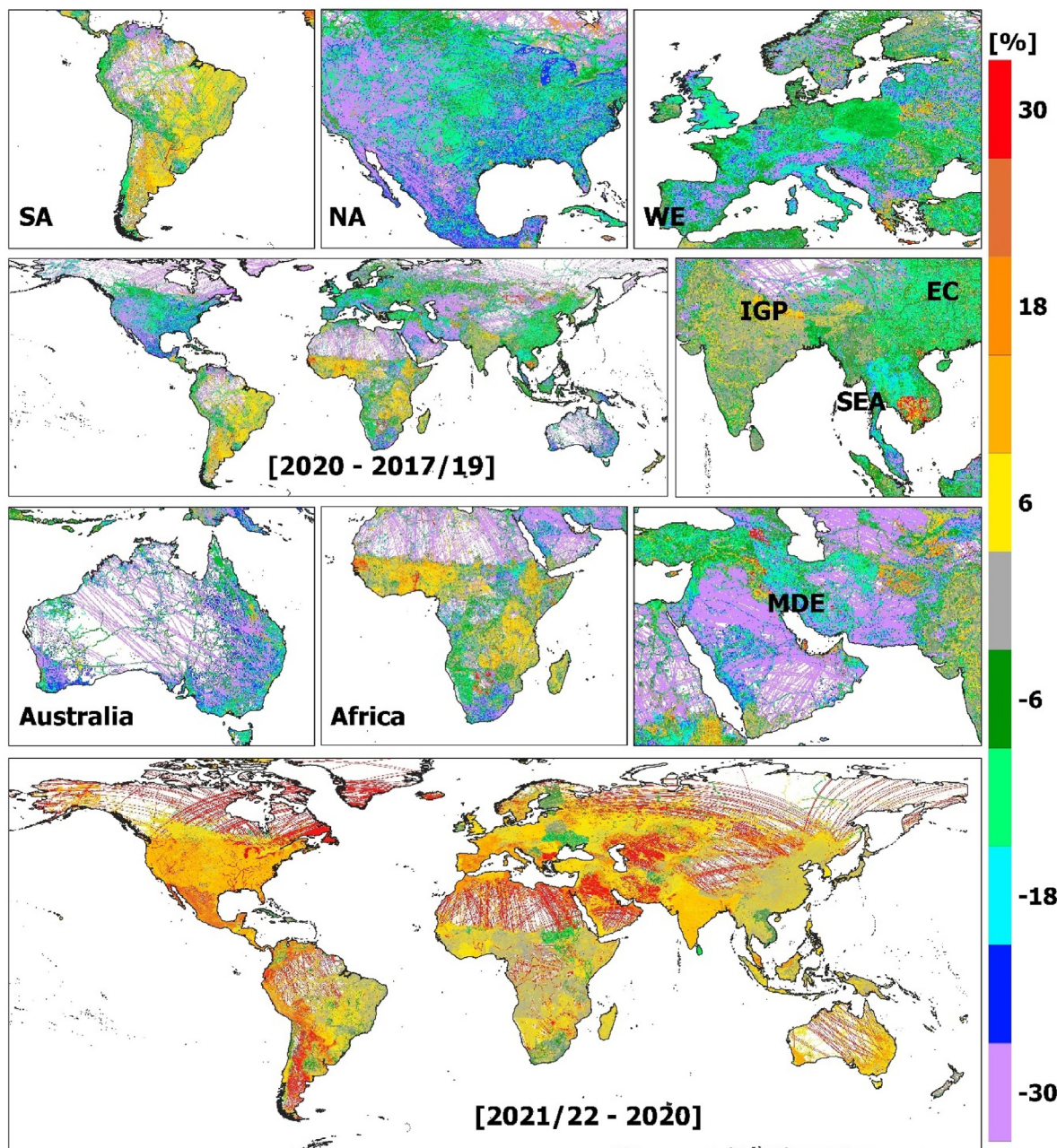


Fig. 5. Changes in SO₂ emission from total anthropogenic activities derived from EGDAR_v8.1 during 2020 compared to 2017–2019 and 2021–2022. Here, the regions are South America (SA), North America (NA), Western Europe (WE), Indo-Gangetic Plain (IGP), East China (EC), Southeast Asia (SEA) and Middle East (MDE).

dominate other anthropogenic sectors in the USA (71 %), Saudi Arabia (70 %), Pakistan (66 %), Mexico (64 %), South Africa (62 %), India (61 %), Indonesia (60 %), Australia (53 %), Russia (50 %), Germany (36 %), Canada (35 %), Spain (35 %) and Italy (31 %). On the other hand, the emissions from manufacturing and construction industry dominate in the UAE (69 %), China (56 %), Brazil (37 %), Japan (32 %), France (31 %) and the UK (23 %). The SO₂ emissions from refinery is also considerable in Central African Republic (23 %), South Africa (19 %), the UK (18 %), Canada (13 %) and Nigeria (8 %). Conversely, we find negligibly small contribution (< 1 %) from road transport to the total anthropogenic emissions in these countries.

During LD, due to restrictions on transport activities the coal consumption is declined in all major coal consumer countries (Fig. 4). The highest decline in coal consumption is found in Spain

(44 %), and then in Mexico (28 %), France (27 %), Italy (27 %), the USA (19 %), Germany (18 %), Canada (16 %), South Africa (12 %), the UK (11 %), Brazil (8 %), India (5 %), Russia (4 %) and Indonesia (3 %). On the other hand, a very small increase in coal consumption is found in China (1.26 %). As coal consumption declined, an improvement in SO₂ pollution is observed in the USA, Canada, Mexico, South Africa, Australia, Spain and Germany, about 1–6 %. Compared to these countries, slightly better improvement in SO₂ pollution is observed in Japan, with its decline of about 6–12 %. On the other hand, despite the reduction in coal consumption, SO₂ is increased in India (1–6 %), Saudi Arabia (1–6 %) and Brazil (6–12 %), which can be due to other sources like AWB and residential emissions that were not stopped during LD.

A decrease or halt in anthropogenic activities like transport or

industries during LD led to a reduction in human-driven SO₂ emissions, as also observed from the inventory, where total emissions decreased during LD compared to PreLD in most regions (Fig. 5). For example, most of the USA, Mexico, MDE, WE, EC, Southeast Asia, Australia and South Africa, including the above-marked hotspot regions, exhibit a decline (6–30 %) in SO₂ emissions, consistent with the changes in SO₂ pollution. Conversely, we observe a slightly different pattern in India. For instance, most regions in IGP show a slight increase in anthropogenic emissions, about 6–18 %. Similarly, there are small or point locations in India that exhibit an increase in SO₂ emissions, about 6–12 %, which well match the slight increase in SO₂ pollution there. Furthermore, a large part of India, including major cities like Delhi, Kolkata and Mumbai, and mining areas in the east, show a decrease in SO₂ emissions of about 6 %. The increase in emissions is also noticeable in a large part of South America, Central Africa and North-western Africa, about 6–18 %. Interestingly, after the ease of lockdown (PostLD) there was a substantial increase (>12 %) in emissions, which also led to a high rise in SO₂ pollution (Fig. 5). This rise is observed in all hotspots and countries mentioned above, but it is more dominant in Mexico, MDE and in the western South America. In summary, the decrease in emissions during LD is mostly attributable to the decrease in human activities, which includes the consumption of coal, as previously mentioned.

3.3. Revisiting the anthropogenic and natural hotspots for effective air pollution mitigation

It is evident from the inventory analysis that most anthropogenic emissions are concentrated in the northern hemisphere. The high amount of SO₂ emitted by human activities is mainly from EC, IGP, Europe, MDE and the USA, and therefore, it declined during LD in these regions. During PostLD when restrictions were lifted, their concentrations reached to the previous year level. This indicates that these regions are mostly controlled by the human-induced SO₂ emissions. It is also evident at the locations of major anthropogenic activities like coal-based thermal power plants and refineries. Density of these industries and associated anthropogenic activities are prominent in the hotspots like the eastern USA, WE, IGP, EC, South Africa and Indonesia (see Fig. 4 and Fig. S3). The high SO₂ pollution in Japan and the southwestern Australia is also anthropogenic, as there are high density of thermal power plants and refineries (Fig. 4). Studies of Krotkov et al. [53] and van der A et al. [54] also showed that SO₂ pollution primarily originates from coal combustion in the north China Plain. Similarly, Kuttippurath et al. [5] showed that thermal power plants, and manufacturing and

construction industries are the major contributors to the SO₂ pollution in IGP and East India. Ukhov et al. [43] suggested that oil refinery, power generation, water desalination, gas flaring and transport activities are the key sources of SO₂ pollution in MDE. It is also evident in changes of SO₂ emission from total anthropogenic activities, as it shows substantial decline in major coal consuming countries during LD. For example, a decline in SO₂ emission of about 13.8 % in the global average, 28.5 % in Canada, 26.4 % in Australia, 23.9 % in Russia, 19.1 % in South Africa, 17.8 % in the UK, 17.6 % in the USA, 17.1 % in China, 14.1 % in France, 8.9 % in Germany, 6.3 % in Japan and 2.3 % in India is observed during LD (Table 2). On the other hand, after the ease of lockdown the anthropogenic emissions increased in these countries. For instance, an increase of about 18.1 % in the global average, 105 % in Australia, 23.1 % in Russia, 18 % in China, 18.4 % in Canada, 15.3 % in the USA, 12.4 % in France, 10.1 % in India, 7.5 % in the United Kingdom, 5.7 % in Germany, 3.6 % in Japan and 0.6 % in South Africa is found during PostLD (Table 2).

However, there are regions where SO₂ pollution is driven by natural activities like forest fires and volcanic eruptions, which were unaffected by LD. Therefore, to find such hotspots, we analyse the land cover dynamics and burnt area, which is a proxy for the burned forest and agriculture area (shown in Fig. S8 and Fig. S9). SO₂ concentrations increased during LD due to the expansion in burned areas in the northern Amazonia, Central Africa, northern Australia and Siberia. Similarly, some regions in Southeast Asia, where biomass burning is intense and are the hotspots of SO₂ pollution, show an increase or no change due to LD. Bush fires in the northern Australia are the main factor that affect air quality [55,56], and show large burned areas there (Fig. S8). A similar situation is found in the countries located in Central Africa and near Amazonia, where an increase in SO₂ pollution is found during LD. Henceforth, these regions are the SO₂ pollution hotspots driven by natural activities.

The enforcement of a complete LD had a profound impact on the air quality across the latitudes [20–22,49,57–60]. The amount of SO₂ emissions from anthropogenic sources decreased substantially, but those from natural sources were comparatively higher during LD. There were reports on improvements in overall air quality and enhanced visibility in major cities because of LD. These changes were associated with improved quality of life and better public health [61,62]. While the current improvements in environmental conditions are temporary, the brief enhancement of air quality during LD serves as an encouraging sign for government authorities and policymakers. It highlights the potential pathways to achieve improved air quality through deliberate and strict restrictions on emission sources in the human driven hotspots. Globally governments may consider implementing targeted LDs in pollution hotspots for specific periods to effectively manage pollution levels in their respective countries or regions while minimising its economic impacts.

Lockdown provided an opportunity for the deteriorated environment and natural resources to recover and regain their health. However, it impeded economic activities, which led to a decline in income, escalating unemployment rates, workforce downsizing, mounting household debt and the overarching economic recession [63]. We observe a decrease in GDP of many countries, such as Japan, Australia, the USA, China, India, France, Germany, the UK, Brazil, South Africa and Russia during the LD period (Fig. S10), which well matches the decline in emissions from total anthropogenic activities in these countries as discussed above. The economic recession was due to a temporary halt in industrial operations, transport activities and human movement caused by the pandemic [64,65]. In addition, the International Energy Agency (IEA) revealed that the anthropause led to a decline of around 5–6

Table 2

Changes in SO₂ total anthropogenic emission derived from EDGAR_v8.1 during lockdown (LD) compared to pre-lockdown (PreLD) and post-lockdown (PostLD) in the global average and different countries.

Country	LD - PreLD [Emission]	PostLD - LD [Emission]
India	-2.3 %	10.1 %
China	17.1 %	18 %
USA	-17.6 %	15.3 %
South Africa	-19.1 %	0.6 %
France	-14.8 %	12.4 %
Germany	-8.9 %	5.7 %
Australia	-26.4 %	105 %
United Kingdom	-17.8 %	7.5 %
Canada	-28.5 %	18.4 %
Nigeria	5.7 %	3.2 %
Japan	-6.3 %	3.6 %
Russia	-23.9 %	23.1 %
Central African Republic	-7.9 %	5.9 %
Global Average	-13.8 %	18.1 %

% in the global energy consumption in 2020 compared to the previous year. The decline in energy consumption during LD is also reported in India, China, France and Germany [22,66]. The significant decline in energy usage resulting from LD measures, played a role in reducing SO₂ emissions from several sectors in many countries, but these sectors play an important role in economic development [67]. For example, a decline in SO₂ emissions from the fossil fuel-based energy and heat power generation sectors was found in China, the USA, the UK, France, Japan, Brazil, Russia, India, South Africa and Germany during LD (Fig. S11).

The decrease in SO₂ emissions in specific sectors stem from the reduction in energy demand, which is also evident in the decrease of coal consumption in these countries during LD (Fig. S11). It is also found from the correlation between coal consumption, sectoral emissions and GDP. For example, the SO₂ emissions from energy and heat power generation show a good correlation with GDP in China (0.53) and Russia (0.64). This is also reflected in the positive correlation between coal consumption and GDP (e.g. Russia). Also, SO₂ pollution from coal consumption shows a positive correlation in India, China and France, with values of 0.82, 0.98 and 0.56, respectively. Other sectorial emissions also degrade environment, as they show a positive correlation with SO₂. We observe a weak and negative correlation between the sectoral emissions and GDP, indicating the importance of other factors in driving economic development. During PostLD, both the economy and emissions increase, highlighting the power of industries and manpower in the economic uplift. This implies the necessity to establish a framework that can stimulate economic growth without compromising air quality. This can be achieved with the adoption of cleaner technologies such as the utilisation of better-quality coal that contains less sulphur, production of more renewable energy, Flue Gas Desulphurisation (FGD) that can reduce SO₂ at source, and stringent environmental norms for both industrial and vehicular emissions [5]. In summary, the anthropause has led to a recess in the economy of many countries, despite an associated improvement in environmental conditions. However, using the LD measures as an example, a new and effective policy can be designed to enhance both the economy and environment.

4. Limitation and future scope

Here, we make use of the reanalysis, satellite measurements and emission inventory for this assessment, but all these are subject to a certain uncertainty. In addition, the EDGAR emission inventory does not consider the emissions from forest fires. Because of this, there can be an uncertainty in the estimated areas of natural emissions. In addition, we have not excluded the influence of meteorological factors on the changes in SO₂ pollution transport during LD. It suggests that the changes in SO₂ during LD cannot solely be attributed to anthropause. Our findings can also be improved with more representative ground-based measurements, satellite observations and regional emission inventory. In addition, there is a need for specific regional studies to find the effectiveness of LD measures for future air quality mitigation plans. On top of these, strict emission standards that are implemented to protect the deteriorating air quality need to be revisited by taking the LD measures as a benchmark.

5. Conclusions

Many cities and regions around the world face poor air quality problems, resulting in many deaths and health issues. Several countries have implemented strict environmental regulations and novel technology to curb air pollution. However, many developing countries still need policies and technologies to improve their air

quality. Therefore, it is important to understand the areas of high pollution, whether it is caused by natural or anthropogenic activities. The COVID-19 LD measures serve as a natural experiment to understand the SO₂ pollution hotspots caused by human or natural activities. The hotspots of IGP, EC, MDE, SA, WE and EUSA are driven by anthropogenic activities such as emissions from fossil fuel burning and industrial operations, where SO₂ pollution is relatively higher ($> 25 \times 10^{-5} \text{ mol/m}^2$). There are also small or point hotspots of SO₂ across the latitudes driven by industries or cities with high human activity. These hotspots are clearly surfaced in the change detection analysis, where there is a decline ($> 10\%$) in SO₂ pollution during LD compared to PreLD. However, during PostLD, the SO₂ pollution reached its previous year level, indicating the need of stringent policies to ensure better air quality.

The SO₂ emissions from energy generation, manufacturing industries and coal consumption also declined in various countries during LD. Although, the anthropause has led to an improvement in SO₂ pollution, there is a decline in the economy during this period. This implies that improving pollution situation during an economic downturn may not be the appropriate course of action, as the livelihoods are heavily dependent on economic conditions. However, we can formulate and design a more effective framework by implementing LD measures, which serve as a potential way forward for stronger economy and improved environmental conditions. This can be achieved by the adoption of cleaner and more advanced technologies, and stringent environmental regulations, which can mitigate air pollution without compromising economic development. The measures implemented during LD could aid in the formulation and revision of existing policies aimed at curbing air pollution in the regions, where human activities are very high. Henceforth, this study unravels the human-made SO₂ hotspots for better global air pollution mitigation strategies and policies.

Funding statement

This study received no funding.

Data availability

Satellite SO₂ Data: <https://sentinels.copernicus.eu/web/sentinel/missions/sentinel-5p/data-products>

EDGAR Data: <https://edgar.jrc.ec.europa.eu/>

Burned area data: <https://cds.climate.copernicus.eu/cdsapp#!/dataset/satellite-fire-burned-area>

Coal Consumption Data: <https://yearbook.enerdata.net/coallignite/coal-world-consumption-data.html>

Location of thermal power plant and refinery: <https://globalenergymonitor.org/download-data-success/>

GDP data: <https://data.worldbank.org/indicator/NY.GDP.MKTP.CD>

Declaration of competing interest

The authors declare that they have no known competing financial interests or personal relationships that could have appeared to influence the work reported in this paper.

CRediT authorship contribution statement

Amritha S: Writing – original draft, Visualization, Validation, Software, Methodology, Formal analysis, Data curation. **Patel VK:** Writing – review & editing, Visualization, Validation, Software, Methodology, Formal analysis, Data curation, Conceptualization. **Kuttipurath J:** Writing – review & editing, Visualization, Validation, Supervision, Resources, Project administration, Methodology,

Investigation, Funding acquisition, Conceptualization. **Varikoden Hamza:** Writing – review & editing, Visualization, Validation, Supervision, Resources, Project administration, Methodology, Investigation, Funding acquisition, Conceptualization.

Acknowledgements

We thank the satellite and ground-based data providers. We also thank the HYSPLIT model developers and the EDGAR emission inventory. We also extend our gratitude to our institutes Department of Physical Oceanography, Kerala University of Fisheries and Ocean Studies Kochi, Indian Institute of Tropical Meteorology, Ministry of Earth Sciences, Pune, CORAL, Indian Institute of Technology Kharagpur for facilitating this study. JK express his gratitude to SERB (CRG/2021/007415) for facilitating the study. We acknowledge the Global Energy Monitor team for maintaining and providing a data for the location of thermal power plant and refineries in the world. We also thanks to the Enerdata for the coal consumption data.

Appendix A. Supplementary data

Supplementary data to this article can be found online at <https://doi.org/10.1016/j.glt.2024.06.003>.

References

- [1] EPA, Integrated Science Assessment for Oxides of Nitrogen—Health Criteria (2016 Final Report), US Environmental Protection Agency, Washington, D.C., 2016. EPA/600/R-15/068, <https://cfpub.epa.gov/ncea/isa/recordisplay.cfm?deid=310879>.
- [2] L.H. Seinfeld, S.N. Pandis, *Atmospheric Chemistry and Physics: from Air Pollution to Climate Change*, John Wiley & Sons, 2016.
- [3] P. Orellano, J. Reynoso, N. Quaranta, Short-term exposure to sulphur dioxide (SO₂) and all-cause and respiratory mortality: a systematic review and meta-analysis, *Environ. Int.* 150 (2021) 106434, <https://doi.org/10.1016/j.envint.2021.106434>.
- [4] V.E. Fioletov, C.A. McLinden, N. Krotkov, C. Li, J. Joiner, N. Theys, S. Carn, M.D. Moran, A global catalogue of large SO₂ sources and emissions derived from the Ozone Monitoring Instrument, *Atmos. Chem. Phys.* 16 (2016) 11497–11519, <https://doi.org/10.5194/acp-16-11497-2016>.
- [5] J. Kuttipurath, V.K. Patel, M. Pathak, A. Singh, Improvements in SO₂ pollution in India: role of technology and environmental regulations, *Environ. Sci. Pollut. Res.* 29 (2022) 78637–78649, <https://doi.org/10.1007/s11356-022-21319-2>.
- [6] A. Robock, L. Oman, G.L. Stenchikov, Regional climate responses to geoengineering with tropical and Arctic SO₂ injections, *J. Geophys. Res. Atmos.* 113 (2008) D16101, <https://doi.org/10.1029/2008JD010050>.
- [7] T.Y. Chiang, T.H. Yuan, R.H. Shie, C.F. Chen, C.C. Chan, Increased incidence of allergic rhinitis, bronchitis and asthma, in children living near a petrochemical complex with SO₂ pollution, *Environ. Int.* 96 (2016) 1–7, <https://doi.org/10.1016/j.envint.2016.08.009>.
- [8] J. Cofala, M. Amann, F. Gyarfas, W. Schoepp, J.C. Boudri, L. Hordijk, C. Kroese, L. Junfeng, D. Lin, T.S. Panwar, S. Gupta, Cost-effective control of SO₂ emissions in Asia, *J. Environ. Manag.* 72 (2004) 149–161, <https://doi.org/10.1016/j.jenvman.2004.04.009>.
- [9] B. Zheng, D. Tong, M. Li, F. Liu, C. Hong, G. Geng, H. Li, X. Li, L. Peng, J. Qi, L. Yan, Y. Zhang, H. Zhao, Y. Zheng, K. He, Q. Zhang, Trends in China's anthropogenic emissions since 2010 as the consequence of clean air actions, *Atmos. Chem. Phys.* 18 (2018) 14095–14111, <https://doi.org/10.5194/acp-18-14095-2018>.
- [10] Z. Klimont, S.J. Smith, J. Cofala, The last decade of global anthropogenic sulfur dioxide: 2000–2011 emissions, *Environ. Res. Lett.* 8 (2013) 014003, <https://doi.org/10.1088/1748-9326/8/1/014003>.
- [11] W. Aas, A. Mortier, V. Bowerox, R. Cherian, G. Faluvegi, H. Fagerli, J. Hand, Z. Klimont, C. Galy-Lacaux, C.M.B. Lehmann, C.L. Myhre, G. Myhre, D. Olivie, K. Sato, J. Quaas, P.S.P. Rao, M. Schulz, D. Shindell, R.B. Skeie, A. Stein, T. Takemura, S. Tsyro, R. Vet, X. Xu, Global and regional trends of atmospheric sulfur, *Sci. Rep.* 9 (2019) 953, <https://doi.org/10.1038/s41598-018-37304-0>.
- [12] M. Coccia, New directions of technologies pointing the way to a sustainable global society, *Sustain. Futures* 5 (2023) 100114, <https://doi.org/10.1016/j.sfr.2023.100114>.
- [13] C.A. McLinden, V. Fioletov, M.W. Shephard, N. Krotkov, C. Li, R.V. Martin, M.D. Moran, J. Joiner, Space-based detection of missing sulfur dioxide sources of global air pollution, *Nat. Geosci.* 9 (2016) 496–500, <https://doi.org/10.1038/ngeo2724>.
- [14] S. Dahiya, L. Myllyvirta, Global SO₂ emission hotspot database – ranking the world's worst sources of SO₂ pollution, *Greenpeace Environment Trust* (2019) 1–13.
- [15] M. Coccia, How do low wind speeds and high levels of air pollution support the spread of COVID-19? *Atmos. Pollut. Res.* 12 (2021) 437–445, <https://doi.org/10.1016/j.apr.2020.10.002>.
- [16] M. Coccia, The effects of atmospheric stability with low wind speed and of air pollution on the accelerated transmission dynamics of COVID-19, *Int. J. Environ. Stud.* 78 (2021) 1–27, <https://doi.org/10.1080/00207233.2020.180293701>.
- [17] R.S. Sokhi, V. Singh, X. Querol, S. Finardi, A.C. Targino, M. de Fatima Andrade, et al., A global observational analysis to understand changes in air quality during exceptionally low anthropogenic emission conditions, *Environ. Int.* 157 (2021) 106818, <https://doi.org/10.1016/j.envint.2021.106818>.
- [18] M. Coccia, The relation between length of lockdown, numbers of infected people and deaths of COVID-19, and economic growth of countries: lessons learned to cope with future pandemics similar to COVID-19, *Sci. Total Environ.* 775 (2021) 145801, <https://doi.org/10.1016/j.scitotenv.2021.145801>.
- [19] J. Kuttipurath, V.K. Patel, R. Kashyap, A. Singh, C. Clerbaux, Anomalous increase in global atmospheric ammonia during COVID-19 lockdown: need policies to curb agricultural emissions, *J. Clean. Prod.* 434 (2023) 140424, <https://doi.org/10.1016/j.jclepro.2023.140424>.
- [20] M. Pathak, V.K. Patel, J. Kuttipurath, Spatial heterogeneity in global atmospheric CO during the COVID-19 lockdown: implications for global and regional air quality policies, *Environ. Pollut.* 335 (2023) 122269, <https://doi.org/10.1016/j.envpol.2023.122269>.
- [21] V.K. Patel, J. Kuttipurath, R. Kashyap, Increased global cropland greening as a response to the unusual reduction in atmospheric PM_{2.5} concentrations during the COVID-19 lockdown period, *Chemosphere* 358 (2024) 142147, <https://doi.org/10.1016/j.chemosphere.2024.142147>.
- [22] J. Kuttipurath, V.K. Patel, G.P. Gopikrishnan, H. Varikoden, Changes in air quality, Meteorology and energy consumption during the COVID-19 lockdown and unlock periods in India, *Air Water Pollut. Rep.* 1 (2023) 125–138, <https://doi.org/10.3390/air1202010>.
- [23] R. Barouki, M. Kogevinas, K. Audouze, K. Belesova, A. Bergman, L. Birnbaum, et al., HERA-COVID-19 working group., Electronic address, The COVID-19 pandemic and global environmental change: emerging research needs, *Environ. Int.* 146 (2021) 106272, <https://doi.org/10.1016/j.envint.2020.106272>.
- [24] L. Ang, E. Hernández-Rodríguez, V. Cyriaque, X. Yin, COVID-19's environmental impacts: challenges and implications for the future, *Sci. Total Environ.* 899 (2023) 165581, <https://doi.org/10.1016/j.scitotenv.2023.165581>.
- [25] Y. Han, X. Gu, C. Lin, M. He, Y. Wang, Effects of COVID-19 on coastal and marine environments: aggravated microplastic pollution, improved air quality, and future perspective, *Chemosphere* 355 (2024) 141900, <https://doi.org/10.1016/j.chemosphere.2024.141900>.
- [26] N.H. Oral, O. Ozdemir, The impacts of COVID-19 lockdown on PM10 and SO₂ concentrations and association with human mobility across Turkey, *Environ. Res.* 197 (2021) 111018, <https://doi.org/10.1016/j.envres.2021.111018>.
- [27] Ö.N. Çalik, Ş.C. Doğruparmak, Effect of COVID-19 lockdown on ambient air quality, *Clean* (2024) e2300101, <https://doi.org/10.1002/cle.202300101>.
- [28] A.P. Akan, M. Coccia, Changes of air pollution between countries because of lockdowns to face COVID-19 pandemic, *Appl. Sci.* 12 (2022) 12806, <https://doi.org/10.3390/app122412806>.
- [29] C. Ling, Y. Li, Substantial changes of gaseous pollutants and health effects during the COVID-19 lockdown period across China, *GeoHealth* 5 (2021) e2021GH000408, <https://doi.org/10.1029/2021GH000408>.
- [30] S. Wang, Y. Zhu, J.C. Jang, M. Jiang, D. Yue, L. Zhong, Y. Yuan, M. Zhang, Z. You, Modeling assessment of air pollution control measures and COVID-19 pandemic on air quality improvements over Greater Bay Area of China, *Sci. Total Environ.* 926 (2024) 171951, <https://doi.org/10.1016/j.scitotenv.2024.171951>.
- [31] F. Qayyum, S. Tariq, H. Nawaz, Z. ul-Haq, U. Mahmood, Z.B. Babar, Variation of air pollutants during COVID-19 lockdown phases in the mega-city of Lahore (Pakistan); Insights into meteorological parameters and atmospheric chemistry, *Acta Geophys.* 72 (2024) 2083–2096, <https://doi.org/10.1007/s11600-023-01208-z>.
- [32] R. Kandari, A. Kumar, COVID-19 pandemic lockdown: effects on the air quality of South Asia, *Environ. Sustain.* 4 (2021) 543–549, <https://doi.org/10.1007/s42398-020-00154-6>.
- [33] B.P. Singh, A. Nair, S. Kumari, S. Kumari, K. Kuamr, J. Gupta, Potential changes in air pollution associated with challenges over South Asia during COVID-19: a brief review, *Asia Pac. J. Atmos. Sci.* 60 (2024) 211–230, <https://doi.org/10.1007/s13143-023-00348-y>.
- [34] Z.S. Venter, K. Aunan, S. Chowdhury, J. Lelieveld, Air pollution declines during COVID-19 lockdowns mitigate the global health burden, *Environ. Res.* 192 (2021) 110403, <https://doi.org/10.1016/j.envres.2020.110403>.
- [35] A.M.D. Navaratnam, H. Williams, S.J. Sharp, J. Woodcock, H. Khreis, Systematic review and meta-analysis on the impact of COVID-19 related restrictions on air quality in low- and middle-income countries, *Sci. Total Environ.* 908 (2024) 168110, <https://doi.org/10.1016/j.scitotenv.2023.168110>.
- [36] R. Gelaro, W. McCarty, M.J. Suárez, R. Todling, A. Molod, L. Takacs, et al., The modern-era retrospective analysis for research and applications, version 2 (MERRA-2), *J. Clim.* 30 (2017) 5419–5454, <https://doi.org/10.1175/JCLI-D-16-0758.1>.
- [37] J.P. Veefkind, I. Aben, K. McMullan, H. Förster, J. De Vries, G. Otter, J. Class, H.J. Eskes, J.F. de Haan, Q. Kleipool, M. van Weele, O. Hasekamp, R. Hoogeveen,

- J. Landgraf, R. Snel, P. Tol, P. Ingmann, R. Voors, B. Kruizinga, R. Vink, H. Visser, P.F. Levelt, TROPOMI on the ESA Sentinel-5 Precursor: a GMES mission for global observations of the atmospheric composition for climate, air quality and ozone layer applications, *Remote Sens. Environ.* 120 (2012) 70–83, <https://doi.org/10.1016/j.rse.2011.09.027>.
- [38] M. Crippa, D. Guizzardi, F. Pagani, M. Schiavina, M. Melchiorri, E. Pisoni, F. Graziosi, M. Muntean, J. Maes, L. Dijkstra, M. Van Damme, L. Clarisse, P. Coheur, Insights on the spatial distribution of global, national and sub-national GHG emissions in EDGARv8.0, *Earth Syst. Sci. Data Discuss.* (2023), <https://doi.org/10.5194/essd-2023-514> [preprint].
- [39] S. Carn, V. Fioletov, C. McLinden, C. Li, N.A. Krotkov, A decade of global volcanic SO₂ emissions measured from space, *Sci. Rep.* 7 (2017) 44095, <https://doi.org/10.1038/srep44095>.
- [40] M.M.M.F. Jion, J.N. Jannat, M.Y. Mia, M.A. Ali, M.S. Islam, S.M. Ibrahim, S.C. Pal, A. Islam, A. Sarker, G. Malafaia, M. Bilal, A.R.M.T. Islam, A critical review and prospect of NO₂ and SO₂ pollution over Asia: hotspots, trends, and sources, *Sci. Total Environ.* 876 (2023) 162851, <https://doi.org/10.1016/j.scitotenv.2023.162851>.
- [41] S. Yan, G. Wu, SO₂ emissions in China – their network and hierarchical structures, *Sci. Rep.* 7 (2017) 46216, <https://doi.org/10.1038/srep46216>.
- [42] T. Wang, P. Wang, N. Theys, D. Tong, F. Hendrick, Q. Zhang, M. Van Roozendael, Spatial and temporal changes in SO₂ regimes over China in the recent decade and the driving mechanism, *Atmos. Chem. Phys.* 18 (2018) 18063–18078, <https://doi.org/10.5194/acp-18-18063-2018>.
- [43] A. Ukhov, S. Mostamandi, A. Da Silva, J. Flemming, Y. Alshehri, I. Shevchenko, G. Stenchikov, Assessment of natural and anthropogenic aerosol air pollution in the Middle East using MERRA-2, CAMS data assimilation products, and high-resolution WRF-Chem model simulations, *Atmos. Chem. Phys.* 20 (2020) 9281–9310, <https://doi.org/10.5194/acp-20-9281-2020>.
- [44] S. Osipov, S. Chowdhury, J.N. Crowley, I. Tadic, F. Drewnick, S. Borrmann, P. Eger, F. Fachinger, H. Fischer, E. Predybaylo, M. Fnais, H. Harder, M. Pikridas, P. Vouterakos, A. Pozzer, J. Sciaire, A. Ukhov, G.L. Stenchikov, J. Williams, J. Lelieveld, Severe atmospheric pollution in the Middle East is attributable to anthropogenic sources, *Commun. Earth Environ.* 3 (2022) 203, <https://doi.org/10.1038/s43247-022-00514-6>.
- [45] M. Li, Z. Klimont, Q. Zhang, R.V. Martin, B. Zheng, C. Heyes, J. Cofala, Y. Zhang, K. He, Comparison and evaluation of anthropogenic emissions of SO₂ and NO_x over China, *Atmos. Chem. Phys.* 18 (2018) 3433–3456, <https://doi.org/10.5194/acp-18-3433-2018>.
- [46] M. Usmani, A. Kondal, J. Wang, A. Jutla, Environmental association of burning agricultural biomass in the Indus River basin, *GeoHealth* 4 (2020) e2020GH000281, <https://doi.org/10.1029/2020GH000281>.
- [47] Y. Hang, F. Wang, B. Su, Y. Wang, W. Zhang, Q. Wang, Multi-region multi-sector contributions to drivers of air pollution in China, *Earth's Future* 9 (2021) e2021EF00212, <https://doi.org/10.1029/2021EF00212>.
- [48] P.S. Rickly, H. Guo, P. Campuzano-Jost, J.L. Jimenez, G.M. Wolfe, R. Bennett, et al., Emission factors and evolution of SO₂ measured from biomass burning in wildfires and agricultural fires, *Atmos. Chem. Phys.* 22 (2022) 15603–15620, <https://doi.org/10.5194/acp-22-15603-2022>.
- [49] M.J. Cooper, R.V. Martin, M.S. Hammer, P.F. Levelt, P. Veefkind, L.N. Lamsal, N.A. Krotkov, J.R. Brook, C.A. McLinden, Global fine-scale changes in ambient NO₂ during COVID-19 lockdowns, *Nature* 601 (2022) 380–387, <https://doi.org/10.1038/s41586-021-04229-0>.
- [50] S. Arora, K.D. Bhaukhandi, P.K. Mishra, Coronavirus lockdown helped the environment to bounce back, *Sci. Total Environ.* 742 (2020) 140573, <https://doi.org/10.1016/j.scitotenv.2020.140573>.
- [51] E.A. Mack, S. Agrawal, S. Wang, The impacts of the COVID-19 pandemic on transportation employment: a comparative analysis, *Transp. Res. Interdiscip. Perspect.* 12 (2021) 100470, <https://doi.org/10.1016/j.trip.2021.100470>.
- [52] E. Mogaji, I. Adekunle, S. Aririguzoh, A. Oginni, Dealing with impact of COVID-19 on transportation in a developing country: insights and policy recommendations, *Transport Pol.* 116 (2022) 304–314, <https://doi.org/10.1016/j.tranpol.2021.12.002>.
- [53] N.A. Krotkov, C.A. McLinden, C. Li, L.N. Lamsal, E.A. Celarier, S.V. Marchenko, W.H. Swartz, E.J. Bucsela, J. Joiner, B.N. Duncan, K.F. Boersma, J.P. Veefkind, P.F. Levelt, V.E. Fioletov, R.R. Dickerson, H. He, Z. Lu, D.G. Streets, Aura OMI observations of regional SO₂ and NO₂ pollution changes from 2005 to 2015, *Atmos. Chem. Phys.* 16 (2016) 4605–4629, <https://doi.org/10.5194/acp-16-4605-2016>.
- [54] R.J. van der A, B. Mijling, J. Ding, M.E. Koukoli, F. Liu, Q. Li, H. Mao, N. Theys, Cleaning up the air: effectiveness of air quality policy for SO₂ and NO_x emissions in China, *Atmos. Chem. Phys.* 17 (2017) 1775–1789, <https://doi.org/10.5194/acp-17-1775-2017>.
- [55] A.M. Graham, K.J. Pringle, R.J. Pope, S.R. Arnold, L.A. Conibear, H. Burns, R. Rigby, N.B. Arriagada, E.W. Butt, L. Kiely, C. Reddington, D.V. Spracklen, M.T. Woodhouse, C. Knote, J.B. McQuaid, Impact of the 2019/2020 Australian megafires on air quality and health, *GeoHealth* 5 (2021) e2021GH000454, <https://doi.org/10.1029/2021GH000454>.
- [56] M. Li, F. Shen, X. Sun, 2019–2020 Australian bushfire air particulate pollution and impact on the South Pacific Ocean, *Sci. Rep.* 11 (2021) 12288, <https://doi.org/10.1038/s41598-021-91547-y>.
- [57] R. Bao, A. Zhang, Does lockdown reduce air pollution? Evidence from 44 cities in northern China, *Sci. Total Environ.* 731 (2020) 139052, <https://doi.org/10.1016/j.scitotenv.2020.139052>.
- [58] S.K. Pani, N.H. Lin, S. RavindraBabu, Association of COVID-19 pandemic with meteorological parameters over Singapore, *Sci. Total Environ.* 740 (2020) 140112, <https://doi.org/10.1016/j.scitotenv.2020.140112>.
- [59] S. Saadat, D. Rawtani, C.M. Hussain, Environmental perspective of COVID-19, *Sci. Total Environ.* 728 (2020) 138870, <https://doi.org/10.1016/j.scitotenv.2020.138870>.
- [60] S. Sharma, M. Zhang, J. Gao, H. Zhang, S.H. Kota, Effect of restricted emissions during COVID-19 on air quality in India, *Sci. Total Environ.* 728 (2020) 138878, <https://doi.org/10.1016/j.scitotenv.2020.138878>.
- [61] L.W.A. Chen, L.C. Chien, Y. Li, G. Lin, Nonuniform impacts of COVID-19 lockdown on air quality over the United States, *Sci. Total Environ.* 745 (2020) 141105, <https://doi.org/10.1016/j.scitotenv.2020.141105>.
- [62] G. He, Y. Pan, T. Tanaka, The short-term impacts of COVID-19 lockdown on urban air pollution in China, *Nat. Sustain.* 3 (2020) 1005–1011, <https://doi.org/10.1038/s41893-020-0581-y>.
- [63] World Bank, *World Development Report 2022: Finance for an Equitable Recovery*, 2022.
- [64] Y. Shang, H. Li, R. Zhang, Effects of pandemic outbreak on economies: evidence from business history context, *Front. Public Health* 9 (2021) 632043, <https://doi.org/10.3389/fpubh.2021.632043>.
- [65] W. Yamaka, S. Lomwanawong, D. Magel, P. Maneejuk, Analysis of the lockdown effects on the economy, environment, and COVID-19 spread: lesson learnt from a global pandemic in 2020, *Int. J. Environ. Res. Publ. Health* 19 (2022) 12868, <https://doi.org/10.3390/ijerph1912868>.
- [66] P. Jiang, Y. Van Fan, J.J. Klemeš, Impacts of COVID-19 on energy demand and consumption: challenges, lessons and emerging opportunities, *Appl. Energy* 285 (2021) 116441, <https://doi.org/10.1016/j.apenergy.2021.116441>.
- [67] IEA, *Government Energy Spending Tracker*, IEA, Paris, 2023. <https://www.iea.org/reports/government-energy-spending-tracker-2>. Licence: CC BY 4.0.